Electronic structure of different Pt-Cu surfaces

M. L. Shek, P. M. Stefan,* I. Lindau, and W. E. Spicer
Stanford Electronics Laboratories, Stanford University, Stanford, California 94305
(Received 2 September 1982; revised manuscript received 10 January 1983)

Soft-x-ray photoemission experiments, utilizing the existence of the Cooper minimum in the Pt $5d$ photoionization cross section, have demonstrated that the widths and peak shapes of the Cu $3d$—derived states of different Pt-Cu surfaces vary according to the atomic coordination between Cu and Pt atoms. For the surface with the largest atomic coordination, namely, the PtCu(111) surface, strong Pt $5d$—Cu $3d$ hybridization is suggested to exist between ~ -1.4 eV and the Fermi level. The feature attributed to such hybridization has a strength which depends on Pt-Cu nearest neighbors in the first approximation. The energy shifts of these Pt—*Cu* $3d$ centroids, relative to pure Cu, seem to correlate with the Pt—*Cu* $2p_{3/2}$ core-level shifts observed with conventional x-ray excitation.

I. INTRODUCTION

We have performed exploratory photoemission experiments to investigate the electronic structures of Pt-Cu surfaces. In addition, it is hoped that an understanding of the Pt-Cu electronic interactions will have implications for two other problems: (1) the electronic factor in the surface segregation phenomenon and (2) the interplay between chemisorption and the electronic structure.

To investigate the Pt $5d$—Cu $3d$ valence band, our method is to utilize the difference in the Pt $5d$ and Cu $3d$ photoionization cross sections and to study different geometrical situations of Pt—Cu bonding. Our approach has the following basis. First, there is a distinctive difference in the photon energy dependence of the Pt $5d$ and Cu $3d$ photoionization cross sections. As will be seen in the next section, the Pt $5d$ emission has a Cooper minimum[1–4] at a photon energy of 150 eV, at which the Cu $3d$ cross section is still large. Hence, the Pt contribution to the valence band is selectively suppressed and the Cu $3d$—derived "density of states" can be extracted.[5] On the other hand, the Cu-induced changes in the Pt $5d$ states can be observed at photon energies less than 150 eV. Therefore, by varying the photon energy, we can identify the origins of the valence structures. A consideration associated with the range of soft-x-ray photon energy used ($h\nu = 80$—150 eV) is the surface sensitivity ($\lesssim 4$ Å) due to the short escape depth of the photoelectrons.[6] It is thus a near-surface "density of states" which we hope to observe. Second, motivated by the feasibility of extracting the near-surface Cu $3d$—derived states, we wish to see how they may vary according to the environment of the Cu atoms. Since the electronic structure of pure Cu is relatively well understood, this may provide a good starting point for an investigation of the electronic structures of Pt-Cu surfaces. A sensitivity of the Cu electronic structure to its environment, in particular, its atomic coordination with the Pt atoms, may be expected from a simple tight-binding picture. An inherent assumption leading to this expectation is that electron tunneling between a Cu atom and a Pt nearest neighbor is largely unaffected by the number and the type of nearest neighbors. We have used these *a priori* considerations to embark on a comparison between various Pt-Cu surfaces: PtCu(110), PtCu(111), and Pt(111) with epitaxially adsorbed Cu (see Fig. 1). However, our interpretations need not be confined by these *a priori* considerations.

In this work, we have found that the electronic interactions between Pt and Cu are sensitive to atomic coordination. In particular, the Cu $3d$—derived near-surface density of states shows a crude dependence on the number of Pt nearest neighbors. The relevance of this work to the problem of surface segregation is suggested by the different extents of Cu surface segregation in two different crystal orientations of the same $Pt_{0.98}Cu_{0.02}$ alloy.[7–9] This work may also be related to our CO chemisorption studies on different Pt-Cu surfaces.[10,11]

To our knowledge, there has been no experimental comparison between the electronic density of states of different surfaces of a pure metal or an alloy, although surface band narrowing has been reported.[12,13] Angle-resolved photoemission on NiCu (110) and (111) surfaces yield different Cu $3d$ structures,[14] which are also different from the structures

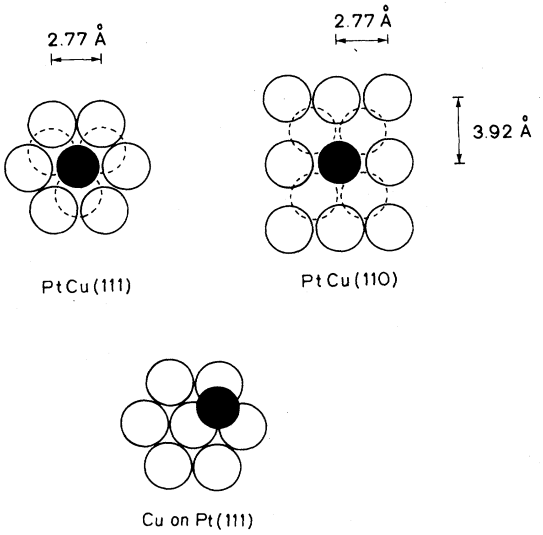

FIG. 1. Nearest-neighbor environment of a Cu atom *in* the top layer of a (111) surface and a (110) surface, and a Cu adatom in one of the possible adsorption sites *on* Pt(111). A filled circle (●) denotes a Cu atom in the top layer. An open circle (○) denotes a Pt atom in the top layer. A broken circle (◌) denotes an atom in the second layer. For low Cu concentrations, Cu-Cu nearest neighbors may be neglected.

observed on the corresponding pure Cu surfaces.[15,16] However, no conclusions can be made about the Cu 3*d* density of states because only small fractions of the Brillouin zones are sampled in angle-resolved photoemission studies. The Cu concentration dependence of the 3*d*-derived states of Pt-Cu surfaces will be seen to be distinctly different from the rather well-studied case of impurity *d* states interacting mainly with the host *sp* bands. For the latter, the energy distribution of the *d* states evolves with *d-d* interactions between like neighbors alone.[17–20]

This paper is organized as follows. The experimental methods will be outlined in Sec. II. The Pt-Cu samples will be described in Sec. III. The photoemission results will be presented in Sec. IV. These include data obtained with soft x-rays from synchrotron radiation as well as x-rays from conventional laboratory sources. The results will be interpreted and discussed in Sec. V. Section VI will be the summary. One aspect of this work, namely, Cu adsorbed on Pt(111), is treated in greater detail elsewhere.[21] For our present purpose, we shall use only the Cu adsorption results which are most relevant to a comparison between various Pt-Cu surfaces.

II. EXPERIMENT

A. General method

Experiments were performed in a stainless-steel vacuum system equipped with a multisample manipulator. The ultimate base pressure after bakeout was 4×10^{-11} Torr. The general procedure for sample cleaning was Ar-ion sputtering and annealing, then oxygen heat cleaning to remove residual carbon, and further annealing *in vacuo*. Ar-ion sputtering was done with 600 eV ion energy and a current density of 1–3 μA/cm^2. Oxygen cleaning was done at around 500 °C, the oxygen partial pressure varying between 5×10^{-9} and 3×10^{-7} Torr according to the extent of carbon contamination. The preparation and characterization of the samples will be described in more detail in Sec. III.

Surface valence-band structures were studied by means of soft-x-ray photoemission spectroscopy. The experiments were performed on the 4° beam line at the Stanford Synchrotron Radiation Laboratory.[22,23] A double-pass cylindrical mirror analyzer was used. The background pressure during the photoemission measurements was typically 1×10^{-10} Torr.

Near-surface compositions were obtained by Auger electron spectroscopy (AES) using a glancing incidence electron beam (2 kV, 3.5 μA). The derivative peak-to-peak height ratios between the Pt 237-eV Auger transition and the Cu 920-eV Auger transition were used to estimate the near-surface Cu concentrations.[24] The relative elemental sensitivity factor was obtained between a pure Pt sample and a thick Cu overlayer on the Pt sample in our own experiments. The surface sensitivity in these AES measurements is 9–11 Å.[25] These AES estimates represent only lower estimates of the surface concentrations.[26]

X-ray photoemission spectroscopy (XPS) on the core levels was performed with a Mg$K\alpha$ source (1253.6 eV, linewidth 0.7 eV) or an Al$K\alpha$ source (1486.6 eV, linewidth 0.8 eV). The vacuum system was also equipped with 4-grid optics for low-energy electron diffraction (LEED).

B. $h\nu$ dependence of Cu 3*d* versus Pt 5*d* photoionization cross sections

In order to identify the Cu 3*d* versus the Pt 5*d* contributions to the valence-band photoemission, we make use of the difference in the photon energy dependence of the Cu 3*d* and Pt 5*d* states. A comparison between the Cu 3*d* and the Pt 5*d* photoionization cross sections is given in Fig. 2. The Cu 3*d* data are obtained with a thick evaporated Cu layer.

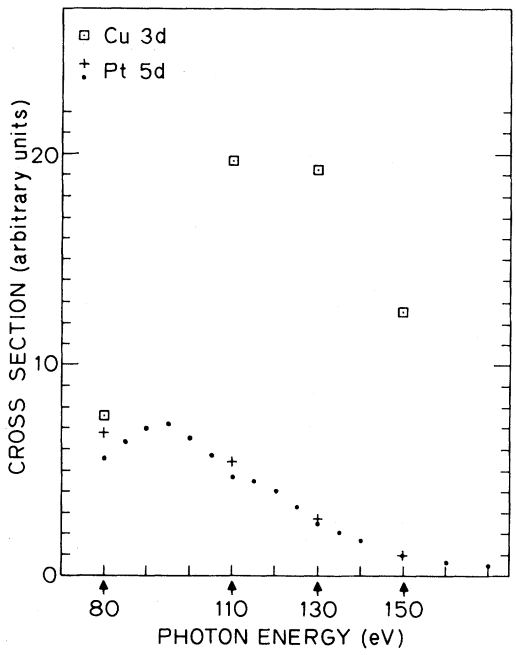

FIG. 2. Comparison between the photoionization cross sections of Pt $5d$ and Cu $3d$ orbitals as a function of photon energy. The Pt $5d$ data from Ref. 4 (●) are normalized so that the cross section at $h\nu=150$ eV is unity. The Pt $5d$ data points from this work (+) are scaled so that the Pt $5d$ cross section is also unity at $h\nu=150$ eV. Our Cu $3d$ data (⊡) were obtained from a thick Cu overlayer. These cross sections represent the emissions integrated over the whole bandwidths, with a linear subtraction of the inelastic contribution. They are not normalized with respect to the number of valence electrons. Corrections have been made for the energy dependence of the analyzer efficiency and the grating transmission.

Our Pt $5d$ data are obtained with a Pt(111) sample. It is seen that the Pt $5d$ cross section rises to a maximum around $h\nu=95$ eV and then drops to a broad minimum starting around $h\nu=150$ eV. As shown by Cooper,[1] the minimum in the cross section is a general occurrence for orbitals with nodes in their radial wave functions.[3,4] On the other hand, for $3d$ orbitals, the cross section merely increases and then decreases. Hence by varying the photon energy, we can crudely identify the orbital origins of the valence structures of the alloy. In particular, by tuning the photon energy to 150 eV, at which the Pt $5d$ Cooper minimum occurs, we can selectively suppress the Pt emission in order to observe the Cu $3d$ states.

The soft-x-ray photoemission data in this work were obtained at these photon energies: 150, 130, 110, and 80 eV. The ratios of Cu $3d$ to Pt $5d$ integrated emissions are respectively 12.5, 7.6, 3.8, and 1.1, with ~15% accuracy.

III. SAMPLES

A. Cu adlayer on Pt(111)

The evaporation of Cu, and the calibration of Cu coverage, on a Pt(111) single-crystal surface are described elsewhere.[21] Here, we only note that the Cu coverage is determined by Auger electron spectroscopy, which, moreover, shows that Cu adsorption on Pt(111) proceeds through a two-dimensional growth mode. Epitaxial adsorption is inferred from LEED.

B. PtCu(110)

The $Pt_{0.98}Cu_{0.02}(110)$ sample was prepared from a single-crystal boule by standard metallurgical techniques. The bulk composition of 2 at.%. Cu and 98 at.% Pt was determined by x-ray microprobe analysis. The details are given elsewhere.[7,9]

The cleaned sample is annealed *in vacuo* at 600 °C till no further Cu surface segregation occurs. The near-surface Cu concentration is 5.9 ± 1.2 at.% as determined by AES. The photoemission data at $h\nu=150$ eV, to be shown later in this paper, yield an estimate of 9.1 ± 2.6 at.% Cu within the top 4 Å of the surface. For the equilibrated surface, a (1×3) LEED pattern is observed. However, a (1×1) surface is easily formed by adsorbing CO at 100 °C. Therefore, it appears possible that the (1×3) surface reconstruction involves only small displacements of the surface atoms from their ideal positions.

C. PtCu(111) surfaces

The PtCu(111) surfaces investigated are not the surfaces of alloys homogenized in the bulk. But they are surfaces formed by thermally diffusing a Cu overlayer into a Pt(111) substrate. The surface sensitivity in our photoemission experiments allows us to use these surfaces obtained after short anneals as model systems for the first few atomic layers of an alloy. The near-surface compositions, determined by AES, are averaged over the escape depth of the Cu 920-eV Auger electrons, or the top 9–11 Å in our detection geometry.

The PtCu(111) soft-x-ray photoemission spectra to be reported were taken in two separate runs. In the first run, over 1 ML (monolayer) of Cu was evaporated on Pt(111). The sample was heated between 540 °C and 610 °C for slightly over 1 min to yield a surface with 15.5 ± 1.5 at.% Cu as determined by

AES. Then the sample was further heated to yield a surface with 7.7±0.7 at % Cu. Using bulk diffusion data for Cu in Pt,[27,28] we may estimate "mean depths of diffusion" which are ~18 and ~38 Å, respectively, for these two surfaces. In the second run, PtCu(111) surfaces of increasing Cu concentrations were formed in cycles. Each cycle consisted of depositing about 1 ML Cu on the Pt(111) surface and heating the sample at 550°C for 1 min. Hence Cu near-surface concentrations of 26.2±1.7, 39.1±2.2, 51.9±2.2, and 59.5±2.2 at. % were obtained after the second, fourth, sixth, and eighth cycle, respectively. An anneal of 550°C for 1 min gives a "mean diffusion depth" of about 11 Å.

In the x-ray photoemission experiment of the Cu $2p_{3/2}$ core level, PtCu(111) surfaces were formed in manners different from those given above. On a Pt(111) surface, ~0.3 ML Cu was evaporated; the sample was heated to 290°C and then the heating current was cut off. From the Cu $2p_{3/2}$ peak area, the Cu surface concentration may be estimated to be 28.5 at. % (surface *X*). It was most likely that the Cu atoms barely started penetrating into the surface, and were distributed in the topmost surface layer as well as on top of the surface. Another PtCu(111) surface was formed by heating a Pt(111) sample covered with >2 ML Cu at ~600°C for 15 min. This gave a near-surface Cu concentration of 12.5 at. % within 6–7.5 Å of the surface as estimated from the Cu $2p_{3/2}$ area (surface *Y*).

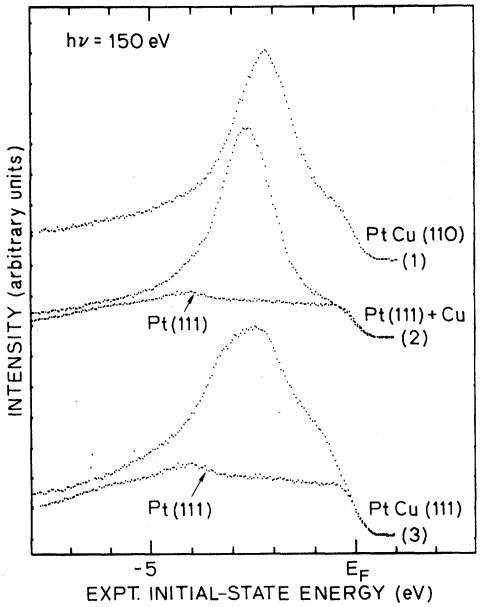

FIG. 3. Valence photoemission spectra obtained at $h\nu = 150$ eV. (1) $Pt_{0.98}Cu_{0.02}(110)$, with 5.9±1.2 at. % Cu as estimated by AES. (2) Pt(111) covered with 0.2 ML Cu. The pure Pt(111) spectrum is also shown. (3) Pt—7.7 at. % Cu(111) surface formed by Cu diffusion into Pt(111). The pure Pt(111) spectrum is plotted on the same scale. All Pt-Cu curves are scaled so that the peak heights are approximately the same.

IV. RESULTS

A. Valence spectra of different Pt-Cu surfaces

We shall show that the Cu 3*d*—derived states are sensitive to the atomic coordination of the Cu constituent of the Pt-Cu surfaces. This is demonstrated by the $h\nu = 150$ eV spectra of surfaces with reasonably dilute Cu concentrations. We shall also make a further comparison between Cu adsorbed on Pt and Cu incorporated into the Pt substrate, with regard to the $h\nu$ dependence of the Cu-induced changes in the valence bands.

Figure 3 shows the $h\nu = 150$ eV spectra of three Pt-Cu surfaces on which the Cu atoms have different coordinations with the Pt nearest neighbors. The Cu concentrations are indicated in the figure caption. It is seen that the PtCu(110) surface gives a sharp peak with a maximum at −2.2 eV (Fermi level E_F defined as zero energy). The Cu-covered Pt(111) surface also gives well-defined peak maximum which, however, lies at −2.6 to −2.7 eV. The diffusion-formed PtCu(111) surface gives a peak which is broader than those on the other two surfaces. The maximum lies around −2.3 to −2.5 eV. The peak is also skewed. These structures are identified as Cu 3*d*—derived, as will be more obvious later when we show the data at other photon energies.

Figure 4 compares the Cu 3*d* states of these Pt-Cu surfaces and contrasts them with the Cu 3*d* band of pure Cu. A crude estimate of the Cu contribution to the PtCu(110) valence spectrum is given by the area above the dashed line associated with curve (1). The full width at half maximum (FWHM) of the Cu 3*d* peak is then estimated to be 1.5–1.6 eV. A slight asymmetry is also apparent on the high-binding-energy side. In Fig. 4, the Cu 3*d* states of Cu on Pt(111) are given by the difference curve between the spectrum of Pt(111) covered with Cu and the spectrum of clean Pt(111). The inelastic contributions have been linearly subtracted before the difference is taken. It is seen that the structure is resonancelike and rather symmetrical, with a FWHM of 1.5 eV. In the following paper we shall show that such a peak shape remains the same up to 0.6–0.7 ML. The 3*d* contribution to the Pt—7.7 at. % Cu(111) spectrum is taken as the difference between the PtCu(111) spectrum and the clean Pt(111) spectrum.

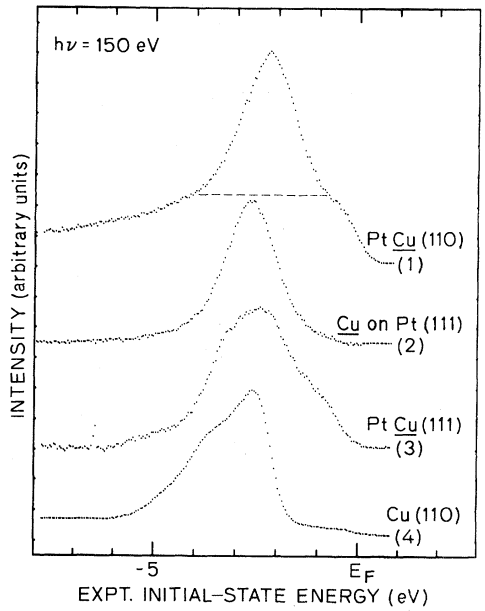

FIG. 4. Comparison of the Cu $3d$—derived valence structure at $h\nu=150$ eV. (1) $Pt_{0.98}Cu_{0.02}(110)$, with 5.9 ± 1.2 at. % Cu as estimated by AES. The area above the broken line indicates an approximate estimate of the Cu $3d$ contribution. (2) Difference between Pt(111) + 0.2 ML Cu spectrum and pure Pt(111) spectrum. (3) Difference between Pt—7.7 at. % Cu(111) spectrum and pure Pt(111) spectrum. (4) Cu(110). All curves are scaled such that the Cu $3d$ contributions have approximately the same intensity.

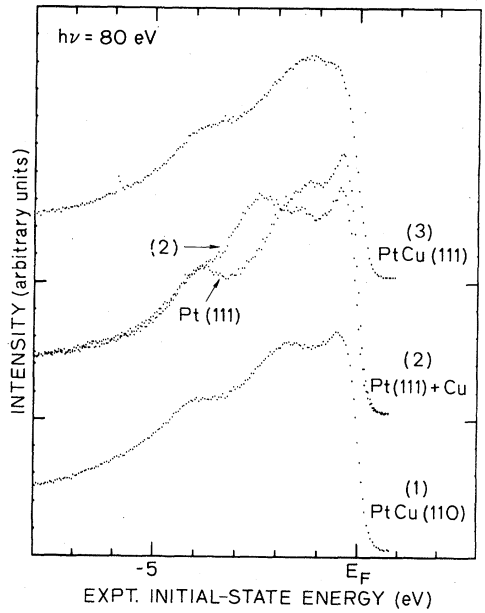

FIG. 5. Valence photoemission spectra obtained at $h\nu=80$ eV. (1) $Pt_{0.98}Cu_{0.02}(110)$, with 5.9 ± 1.2 at. % Cu as estimated by AES. (2) Pt(111) covered with 0.2 ML Cu. The pure Pt(111) spectrum is also shown in the same scale. (3) Pt—7.7 at. % Cu(111) surface formed by Cu diffusion into Pt(111). All Pt-Cu curves are scaled such that the maximum peak heights are approximately the same.

Structures exist on both the high-binding-energy side and the low-binding-energy side of the peak maximum, that is, at -3.1 to -3.2 eV and also between approximately -1.4 eV and the Fermi level. This peak shape is representative of the $3d$ states of a relatively dilute amount of Cu in Pt(111). For the pure Cu spectrum, the dominant d peak lies at -2.6 eV and has a sharp leading edge; structures occur at -3.5 to -3.6 eV and in the region below -4.5 eV. Therefore, we see that the Cu $3d$ states of the different Pt-Cu surfaces are different from not only one another but also from the pure Cu $3d$ states. The general differences between the Pt*Cu* $3d$ states, on the one hand, and the pure Cu $3d$ states, on the other, can be stated as follows. (1) The Pt—*Cu* $3d$ centroids are all shifted towards smaller binding energies relative to the pure Cu $3d$ centroid. These centroid shifts are tabulated in the following paper. (2) At approximately -1.4 eV, where the onset of the dominant d peak in pure Cu occurs, all the Pt—*Cu* $3d$ states already show significant emissions.

Figure 5 shows the valence spectra obtained at $h\nu=80$ eV, where the ratio of Cu $3d$ to Pt $5d$ cross sections is only about 1.1 according to Fig. 2. These spectra serve to illustrate the $h\nu$ dependence of the valence-band features and to confirm the identification of the peak structures observed at $h\nu=150$ eV as Cu $3d$ derived. The greatest change at $h\nu=80$ eV, relative to pure Pt, is that the emissions in the top ~2 eV of the valence bands have greatly decreased for all the Pt-Cu spectra. For Pt— 7.7 at. % Cu(111), the -0.4-eV peak of the pure Pt(111) spectrum is no longer evident. Below ~-2 eV, there is a Cu-induced increase in emission. The changes induced by Cu on Pt(111) and Cu in Pt(111) will be more clearly shown below.

To distinguish between Cu $3d$—derived states and possible Pt $5d$ rearrangement, an examination of the $h\nu$ dependence of the Cu-induced changes is useful. Figure 6 gives a comparison between the difference spectra[29] at several photon energies for the case of Cu on Pt(111) and the case of Cu in Pt(111). For Cu *on* Pt(111) in Fig. 6(a), the difference curve with Pt(111) at $h\nu=130$ eV shows a resonancelike feature similar to that $h\nu=150$ eV. In the difference curve at $h\nu=80$ eV, the negative change between E_F and ~-2 eV has been noted in relation with Fig. 5, the increase in emission below ~-2 eV reflects, to a rather large extent, the Cu-induced increase at $h\nu=130$ and 150 eV. For Cu *in* Pt(111) in Fig. 6(b),

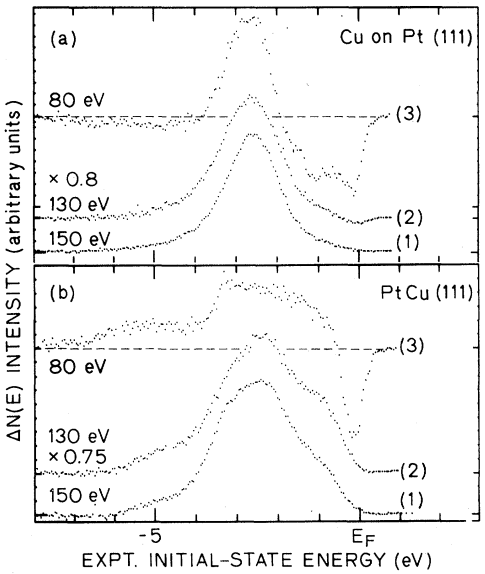

FIG. 6. Comparison of the Cu-induced changes $\Delta N(E)$ at different photon energies. (a) Difference curves between the spectra of Pt(111) + 0.2 ML Cu and pure Pt(111) spectra. (1) to (3): $h\nu=150$, 130, and 80 eV, respectively. (b) Difference curves between Pt—7.7 at. % Cu(111) spectra and pure Pt(111) spectra. (1) to (3): $h\nu=150$, 130, and 80 eV, respectively. In both (a) and (b), curve (2) is scaled so that its dominant peak intensity is roughly the same as that in curve (1), and the multiplication factor is given next to the curve. The text gives the more precise intensity ratios. Curve (3) is shown in the same scale as curve (1). Among each set of curves (1)—(3), corrections to the experimental intensities have been made (corrections due to the energy dependence of analyzer efficiency and the grating transmission). The vertical scales of (a) and (b) are not the same.

the difference curve at $h\nu=130$ eV has a peak shape quite similar to that at $h\nu=150$ eV, with a slightly larger relative increase between -1.4 eV and E_F. At $h\nu=80$ eV, the maximum attenuation occurs at -0.1 to -0.15 eV. Furthermore, below -0.5 eV in the difference curve at $h\nu=80$ eV, there is a broad increase in emission without dominant structures.

B. PtCu(111) valence spectra: Cu concentration and $h\nu$ dependence

There are two general observations to be made about the results to be shown in this section. First, with increasing Cu concentration, the emission between -1.4 eV and E_F increases approximately linearly with Cu concentration up to between 25 and 30 at. %; then it increases much more slowly with higher Cu concentrations. This suggests that this feature is dominated by Pt-Cu rather than Cu-Cu interactions. Second, these data show that the changes between -1.4 eV and E_F have a different $h\nu$ dependence from the changes in the higher-binding-energy region.

Figure 7 presents the PtCu(111) spectra at $h\nu=150$ eV for several Cu concentrations between 26.2 and 59.5 at. %. As the Cu concentrations increase, the emission between -1.4 eV and E_F increases much more slowly than the dominant peak. We also note that the -1.4 eV to E_F emission for these larger Cu concentrations is very much stronger than the pure Pt(111) emission in this energy range.

Figure 8 shows that the total area under the Cu $3d$ peak (approximated by difference spectra) varies linearly with the Cu near-surface concentration estimated with Auger-electron spectroscopy. On the other hand, the emission between -1.4 eV and E_F first increases linearly up to about 26 at. %, after which the rate of increase becomes much smaller. Since the low-binding-energy emission is only a small fraction of the total emission for large Cu concentrations, it cannot be determined whether it is the total emission or the emission of the dominant peak which increases linearly with Cu concentration.

In order to understand the emission between -1.4 eV and E_F observed at $h\nu=150$ eV, we have investigated the valence spectra at several other photon energies. Figures 9 and 10 give the Cu-induced difference spectra from $h\nu=150$—80 eV.[29] In Fig. 9, the results at $h\nu=130$ eV are rather similar to those at $h\nu=150$ eV, and, as the Cu concentration increases, the emission between 1.4 eV and E_F also increases more slowly than the dominant peak. In contrast, the spectra at $h\nu=110$ eV show some qualitative differences with those at $h\nu=150$ and 130 eV; and relatively strong structures exist at ~ -1 eV, especially for 26.2 and 39.1 at. % Cu. In Fig. 10, the

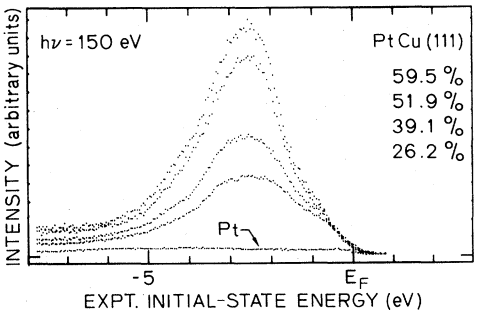

FIG. 7. Valence photoemission spectra of diffusion-formed PtCu(111) surfaces, $h\nu=150$ eV. From bottom curve to top curve: pure Pt(111), Pt—26.2 at. % Cu(111), Pt—39.1 at. % Cu(111), Pt—51.9 at. % Cu(111), and Pt—59.5 at. % Cu(111).

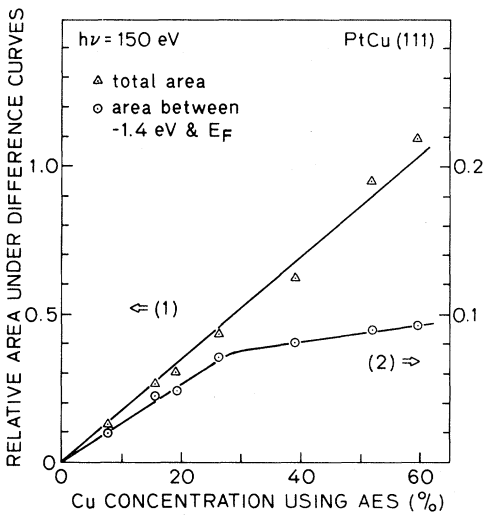

FIG. 8. Strength of Cu-induced structures, at $h\nu=150$ eV, as a function of Cu near-surface concentrations estimated with AES. (1) The total area under each difference curve (△). (2) The area between -1.4 eV and E_F under each difference curve (⊙). Unity area is defined to be the area of the dominant peak (the high binding-energy peak) in the Pt—59.5 at.% Cu(111) difference curve. Note that the vertical scale of curve (1) is on the left and the vertical scale of curve (2) is on the right, as indicated by the arrows.

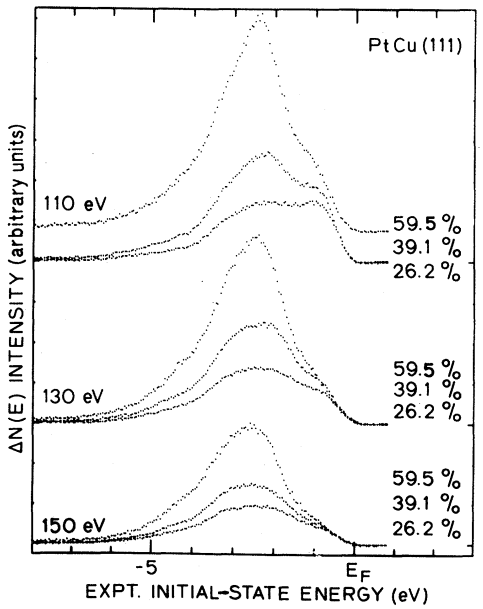

FIG. 9. Cu-induced changes $\Delta N(E)$ in the PtCu(111) valence-band photoemission spectra; $h\nu=150$, 130, and 110 eV. These are difference curves between PtCu(111) spectra and the corresponding Pt(111) spectra. At $h\nu=150$ eV, from bottom to top curve: Pt—26.2 at.% *Cu*(111), Pt—39.1 at.% *Cu*(111), and Pt—51.9 at.% *Cu*(111). At $h\nu=130$ and 110 eV, the same surfaces are shown in the same order from bottom to top. All these curves have the same vertical scale, with corrections made for the energy dependence of analyzer efficiency and grating transmission.

Cu-induced difference spectra at $h\nu=80$ eV show a decreased emission near E_F for all Cu concentrations. Below ~ -0.5 eV, the broad increase for 7.7 at.% Cu develops structures for larger Cu concentrations, and moreover, the structure between -1.4 eV and E_F evolves in a manner distinct from that of the high-binding-energy region below -1.4 eV.

Figure 11 graphically compares, for the difference spectra of 26.2 at.% Cu, the $h\nu$ dependence of the spectral region below -1.4 eV with the region between -1.4 eV and E_F. The integrated areas of the two regions under the difference spectra are compared. For the emission above -1.4 eV in the $h\nu=80$ eV difference spectrum, only the positive contribution is considered. It is seen that the $h\nu$ dependence of the high-binding-energy region below -1.4 eV resembles the $h\nu$ dependence of pure Cu $3d$ emission. In contrast, the emission above -1.4 eV is much larger than a pure Cu $3d$—like emission at $h\nu=110$ eV. Plots for 39.1 and 59.9 at.% Cu can also be derived from Figs. 9 and 10, with qualitatively similar trends as those in Fig. 11.

C. Cu 2*p* core-level shifts

Figure 12 presents the Cu $2p_{3/2}$ core-level spectra on various Pt-Cu surfaces, which may be compared with the Cu $2p_{3/2}$ spectrum of pure Cu and the Cu $2p_{3/2}$ spectrum of a sputtered $Ni_{0.90}Cu_{0.10}(1110)$ surface which is not annealed. A large shift in binding energy (between -0.6 and -1.0 eV) is observed for the Cu $2p_{3/2}$ core levels of all the Pt-Cu surfaces, although small variations do exist between different surfaces. As will be discussed in the following paper, there seems to be a crude correlation between these core-level shifts and the $3d$ centroid shifts relative to the pure Cu $3d$ centroid. The FWHM of the Cu $2p_{3/2}$ core levels are all similar (1.4—1.5 eV).

V. INTERPRETATION AND DISCUSSION

We shall first discuss the sensitivity of the Cu $3d$ states to the surface atomic coordination. We shall then interpret the results on the Cu concentration and $h\nu$ dependence of the PtCu(111) valence spectra, in terms of the Pt $5d$—Cu $3d$ hybridization which depends on Pt-Cu nearest-neighbor interactions to the first approximation. The correlation between

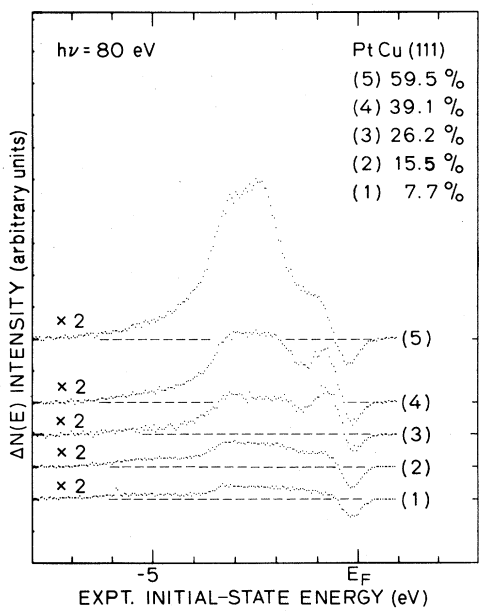

FIG. 10. Cu-induced changes $\Delta N(E)$ in the PtCu(111) spectra obtained at $h\nu=80$ eV. These are difference curves between PtCu(111) spectra and the pure Pt(111) at the same energy. (1) 7.7 at. % Cu. (2) 15.5 at. % Cu. (3) 26.2 at. % Cu. (4) 39.1 at. % Cu. (5) 59.5 at. % Cu. The intensities are magnified by a factor of 2 with respect to the intensities in Fig. 13. Corrections have been made in all these curves for the energy dependence of analyzer efficiency and grating transmission.

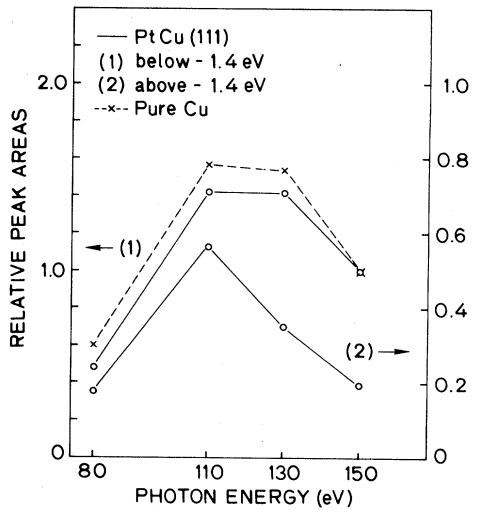

FIG. 11. Comparison of the $h\nu$ dependence of (1) the high-binding-energy region below -1.4 eV with (2) the spectral region between -1.4 eV and E_F, in the difference spectra for 26.2 at. % Cu. Note (1) and (2) have different vertical scales, with the high-binding-energy area obtained at $h\nu=150$ eV defined as unity. The pure Cu $3d$ emission ($\times$) is scaled to unity at $h\nu=150$ eV. The lines in the figure only serve to connect the related data points at various photon energies. Corrections have been made for the energy dependence of analyzer efficiency and grating transmission.

the shifts of the Cu $3d$ centroids and the Cu $2p_{3/2}$ core levels, relative to pure Cu, will be briefly discussed. (The correlation will be discussed further in the following paper.) Lastly, we shall make a comparison with other results.

A. Sensitivity of the valence electronic structure to surface atomic coordination

The differences in the Cu $3d$–derived states on the various Pt-Cu surfaces with dilute Cu concentrations, shown in Fig. 4, can be crudely rationalized by the differences in surface atomic coordination. For a Cu adatom on the Pt(111) surface, it can interact with at most three Pt neighbors. On a fcc(110) face, the atomic coordinations in the top two layers are 7 and 11, respectively. On a fcc(111) face, a Cu atom *in* the top layer may interact with nine Pt neighbor atoms. In the second layer, the bulk coordination number of 12 is already attained. Hence the narrow widths of the $3d$ states of Cu on Pt(111) and of PtCu(110) reflect weak Pt—Cu bonding due to reduced numbers of nearest neighbors. Moreover, the asymmetry noted on the PtCu(110) $3d$ peak, as distinct from the symmetrical shape of the Cu $3d$ peak on the Pt(111), is consistent with the interpretation that there are more Pt—Cu bonding states as the number of Pt neighbors increases. In the broad Cu $3d$ structure associated with PtCu(111), the shoulder around -3.2 eV may be due to the Pt—Cu bonding states whose origin may be similar to that of a shoulder at -3.5 eV in the pure Cu valence spectra (Fig. 4).[30,31] This feature in pure Cu, occurring at about 0.9 eV on the higher-binding-energy side of the $3d$ peak maximum, is attributed to the states near L_3 of the Brillouin zone[30] and part of the t_{2g} projection in the density of states.[32] The emission above -1.4 eV can be attributed to Cu $3d$ electron rearrangement due to hybridization with Pt $5d$ states, as will be shown next.

B. Pt $5d$—Cu $3d$ hybridization

The data in Sec. IV B give support to the interpretation that, in the $h\nu=150$ eV difference spectra between PtCu(111) and Pt(111), the emission between -1.4 eV and E_F is due to Cu $3d$, and not Pt $5d$. The reasons are as follows: (1) At $h\nu=150$ eV, it is seen

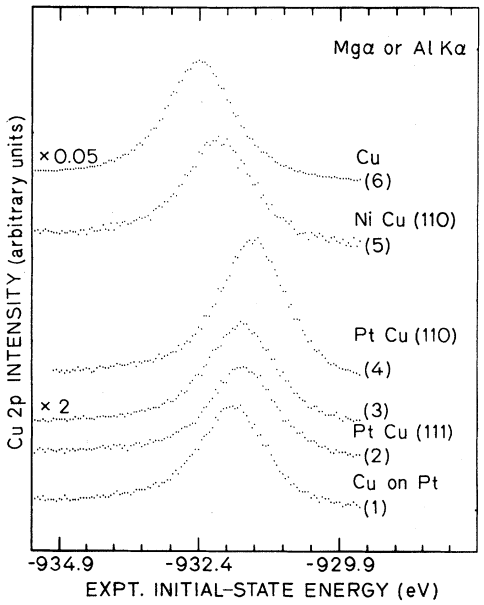

FIG. 12. Comparison of Cu $2p_{3/2}$ of various systems. (1) ~0.3 ML Cu on Pt(111) estimated by AES. (2) Surface X: 28.5 at. % Cu in Pt(111) estimated by XPS. (3) surface Y: 12.5 at. % Cu in Pt(111) estimated by XPS. (4) $Pt_{0.98}Cu_{0.02}(110)$, with 5.9±1.2 at. % Cu estimated by AES. (5) Sputtered $Ni_{0.97}Cu_{0.02}(110)$ with ≤ 10 at. % Cu. (6) Pure Cu(110), multiplied by a factor of 0.05. Curve (3) is observed with Al $K\alpha$ radiation. All the other spectra are taken with Mg $K\alpha$ radiation. The intensity of (3) has been corrected for the difference between using Al $K\alpha$ and Mg $K\alpha$, and then magnified by 2 for display. The energies are defined with respect to E_F.

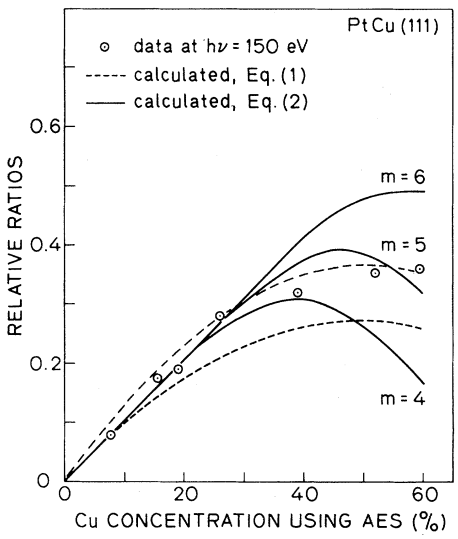

FIG. 13. Cu concentration dependence of the Cu-induced emission between −1.4 eV and E_F observed at $h\nu = 150$ eV: A comparison between experiment and calculations. The experimental data are indicated by (⊙). The curves obtained by calculating the number of Pt–Cu bonds using Eq. (1) are indicated by (— — —). The lower curve (— — —) is matched with the experimental observation at 7.7 at. % Cu, while the upper curve (— — —) is matched with the experimental observation at 26.2 at. % Cu. The curves obtained by calculating the number of Cu atoms with m or fewer like nearest neighbors, using Eq. (2), are shown by (——) with the different m values indicated. Both curves (——) are matched to experimental observation at 7.7 at. % Cu.

that the emission above −1.4 eV is much stronger than the clean Pt(111) emission (Fig. 7). It is unlikely that there should be some sharply rearranged Pt 5d states to account for the strong emission above −1.4 eV in the PtCu(111) spectra. (2) If this Cu-induced feature at $h\nu = 150$ eV were due to rearranged Pt 5d states, then there should be a manifold increase observed at $h\nu = 80$ eV, where the Pt 5d cross section is large. Instead, a decrease in Pt 5d emission between ~−0.5 eV and E_F is observed (Figs. 6 and 10).

It is unlikely that the Cu 3d states between −1.4 eV and E_F should be due to a second Cu species experiencing a different potential. Suppose there were two Cu species, one peaking at ~−2.3 eV and the other at ~−1 eV. Then the difference between ~−2.3 and ~−1 eV would lead to a difference in core-level binding energies of the same order. Yet no noticeable broadening or skewing of the Cu $2p_{3/2}$ core level of PtCu(111) is observed. The width remains similar to those associated with narrow Cu 3d states.

The emission between −1.4 eV and E_F in the Cu 3d–derived density of states ($h\nu = 150$ eV) is likely to arise from Cu 3d–Pt 5d hybridization. The more gradual increase in the strength of the emission, beyond ~26 at. %, can be explained by the increasing number of Cu-Cu nearest neighbors in place of Pt-Cu nearest neighbors. The nature of the variation will be discussed shortly. Moreover, we have shown that the emission above −1.4 eV has a different $h\nu$ dependence compared with the high-binding-energy region below −1.4 eV and with pure Cu 3d states. At $h\nu = 110$ eV, the excessive intensity between −1.4 eV and E_F may be a consequence of some Pt 5d contribution to the valence electronic rearrangement (below −0.5 eV). However, if this is the case, then it seems that the Pt 5d and the Cu 3d contributions are not simply additive. If they were additive, the corresponding emission at $h\nu = 80$ eV would be much higher than the observed emission since the pure Pt 5d emission increases from $h\nu = 110$ to 80 eV.

We now pursue the interpretation that the varia-

tion in the number of Pt-Cu nearest neighbors leads to the observed Cu concentration dependence of the feature associated with Pt $5d$—Cu $3d$ hybridization. We shall compare the strength of this feature, observed at $h\nu=150$ eV, with two different viewpoints of the Pt-Cu nearest-neighbor interactions. The first is to assume that the strength ($S_{\text{Pt-Cu}}$) is governed by the number of Pt-Cu nearest-neighbor pairs. For a random distribution of Cu and Pt atoms,[33] $S_{\text{Pt-Cu}}$ is given by

$$S_{\text{Pt-Cu}} \propto x_{\text{Cu}}(1-x_{\text{Cu}}) , \tag{1}$$

where x_{Cu} is the atomic fraction of Cu. A second possibility is to consider a local cluster of like and unlike nearest neighbors around a Cu atom in a random distribution. Then we ask what is the maximum number (m) of Cu nearest neighbors which the Cu atom in question can tolerate, before it starts to lose hybridization with its Pt neighbors. The strength of the Pt $5d$—Cu $3d$ hybridization feature (S_{Cu}) is taken to be proportional to the number of Cu atoms which can hybridize with Pt:

$$S_{\text{Cu}} \propto x_{\text{Cu}} \sum_{l=0}^{m} \frac{9!}{(9-l)!l!} x_{\text{Cu}}^{l}(1-x_{\text{Cu}})^{9-l} . \tag{2}$$

In Eq. (2), only the topmost layer is considered, and each atom has a coordination number 9, including bonding with the second layer.

The results calculated from either assumption are compared with experimental data in Fig. 13. We have quite arbitrarily chosen to match calculation and experiment at 7.7 at. % Cu, which is the lowest Cu concentration studied. The results calculated from the second assumption are, to a good approximation, linear up to ~26 at. % Cu for a maximum of five to six Cu nearest neighbors.[34] On the other hand, the first assumption yields a nonlinear variation with Cu concentration even at low Cu concentrations. Therfore, fitting experiment and calculation at 7.7 at. % Cu places the calculated curve in a different position compared with the result of fitting at ~26 at. % Cu, as shown in Fig. 13. In spite of uncertainties due to the unknown proportionality constants relating experiment and calculation, the calculations nevertheless yield the first rapid and then slow increase of the Pt $5d$—Cu $3d$ hybridization. The statistics of our data are insufficient to distinguish between the two possibilities. However, regardless of which possibility is correct, the Cu concentration dependence of the Pt $5d$—Cu $3d$ hybridization is explained by Pt-Cu nearest-neighbor interactions in the first approximation. The quantitative deviation of the second assumption from experiment, at Cu concentrations larger than 26 at. % Cu, may be due to the effects of Cu-Cu interactions beyond the nearest-neighbor shell.

C. Correlation between the $3d$ centroid shifts and Cu $2p$ core-level shifts of the Cu component

As noted in Sec. IV C, the energy shifts of the Pt—Cu $3d$ centroids, relative to pure Cu, seem to be correlated with the Pt—*Cu* $2p_{3/2}$ core-level shifts. In the following paper,[21] these and other energy shifts will be tabulated, and compared with the expectations of a thermodynamical model for core-level shifts. It will also be argued that simplistic interpretations in terms of charge transfer between the Pt and the Cu constituents do not hold. Here we only indicate two possible interpretations. (1) The final-state relaxation energy, due to the screening of a $3d$ hole or a $2p$ hole, may be larger on the Pt-Cu surfaces relative to a pure Cu surface. Within the context of the model used in the following paper, this provides the dominant energy shift. (2) Both the $3d$ centroid shifts and the Cu $2p_{3/2}$ core-level shifts may result from a smaller s-d hybridization of the Cu component, compared with that in pure Cu. The increased density of d electrons raises the energies of the $3d$ centroids as well as those of the core levels.[12,35]

D. Comparison with other work on group-VIII—group-*IB* metal alloys

In the following discussion, it must be borne in mind that different experiments may have various surface sensitivities in addition to inherent differences in the samples.

Previous x-ray photoemission experiments on *polycrystalline* PtCu alloys have shown an upward shift of the valence-band centroid, relative to the centroid derived from the weighted sum of the emissions of the pure components.[35] The shift of the valence-band centroid is attributed to the Cu $3d$ component. These findings are not inconsistent with our observations on the near-surface Cu $3d$ states at $h\nu=150$ eV. However, unlike the x-ray photoemission results on the valence bands, our results are not sensitive to possible changes in the centroid of the Pt $5d$ states[36,37] because of the low cross section of the latter at $h\nu=150$ eV. At low Cu concentrations, when the Cu $3d$ emission does not totally dominate, possible changes in the Pt $5d$ centroid are probably small. At high Cu concentrations, the Cu $3d$ emission dominates the valence spectra.

It is interesting to note that, for $Pd_{0.4}Cu_{0.6}$, the Cu valence $\rightarrow L_3$ x-ray emission band consists of a peak with maximum at ~ -2.6 eV and a feature between -2.0 eV and E_F.[38] This indicates that the lo-

cal valence electronic density of states on the Cu atom has significant weight in the energy range where the pure Cu valence electronic density of states is low. It is plausible, then, that this reflects a similarity between the electronic structures of PtCu and PdCu alloys, which is also consistent with their similar Cu core-level binding-energy shifts.[39]

X-ray photoemission experiments show that, for PdCu alloys with 6 and 25 at. % Cu, the difference spectra with respect to pure Pd yield a broad and flat positive emission below -0.5 eV, and a decrease above -0.5 eV.[39] From the flatness of the Cu-induced increase, it has been concluded by the authors that the Cu loses its identity for these low concentrations. We note that these difference spectra resemble the difference spectra for 7.7 and 15.5 at. % Cu in Pt(111) observed at $h\nu=80$ eV. However, we know that the results at other photon energies, namely 130 and 150 eV, show that definite Cu $3d$—derived structures do exist on these surfaces with dilute Cu concentrations. Hence we should regard with caution the suggestion that the d states of dilute concentrations of noble metals will be strongly spread throughout the host d band if there is degeneracy between the noble-metal d states and the host d states. Furthermore, our observations on the distinct Cu $3d$—derived states on Pt(111) and of the $Pt_{0.98}Cu_{0.02}(110)$ surface demonstrate that degeneracy between the impurity d states and the host d band is not a sufficient condition for strong electronic interactions.

For dilute Cu in Ni, the Cu $3d$ states do not form a split-off band but lie at the bottom of the Ni $3d$ band as a broad emission.[19,20] Theoretical calculations are in good agreement on this,[40,41] whether or not they incorporate the randomness of the d-d overlap and s-d hybridization (off-diagonal disorder). However, such randomness becomes significant in alloys between metals which have largely different bandwidths. In PdAg alloys, for instance, no split Ag band is predicted for a dilute Ag concentration (20 at. %) if the only randomness which is considered is that of the different d-scattering resonances (diagonal disorder).[42] This is in contradiction with the observation of Ag d states split from the Pd d states in a 10 at. % Ag alloy.[43–45] On the other hand, a calculation treating both the randomness of the d resonances and the randomness of the d-d as well as s-d interactions shows the existence of a split Ag subband for low Ag concentrations.[46]

The difference between Pt $5d$ resonance and Cu $3d$ resonance is not as large as the difference between Pd $4d$ and Ag $4d$ resonances. However, the much larger Pt-Pt electron hopping relative to the Cu-Cu electron hopping may similarly be an important consideration in understanding the extent of the interactions between Pt and Cu.

VI. SUMMARY

The following is a general summary of the results presented in this paper:

(1) Utilizing the Cooper minimum of the Pt $5d$ emission ($h\nu=150$ eV), we have observed variations in the Cu $3d$ states of different Pt-Cu surfaces which are visualized to have different Pt-Cu nearest-neighbor interactions.

(2) Using a photon energy at which the Pt $5d$ emission is strong ($h\nu=80$ eV), we have observed a decrease in the Pt $5d$ states near E_F when Cu interacts with Pt(111).

(3) The Cu-induced changes of the Pt(111) valence band, approximated by difference curves between PtCu(111) and Pt(111), have been studied in some detail by varying the photon energy and the Cu concentration of PtCu(111). It is found that the changes from ~ -1.4 eV to E_F and the changes below -1.4 eV have a different dependence on photon energy as well as on Cu concentration. The changes in the high-binding-energy region vary as pure Cu $3d$ states. We thus suggest that between -1.4 eV and E_F, there is significant Cu $3d$—Pt $5d$ hybridization. Moreover, this hybridization depends on Pt-Cu nearest-neighbor interactions in the first approximation.

(4) The centroids of the Cu $3d$ states of various Pt-Cu surfaces, for small amounts of Cu are shifted towards smaller binding energy (towards E_F) relative to the pure Cu $3d$ centroid. Similarly, the Cu $2P_{3/2}$ core levels of these Pt-Cu surfaces are shifted towards smaller binding energy relative to the pure Cu $2p_{3/2}$ core level. This will be further discussed in the next paper.

ACKNOWLEDGMENTS

We would like to acknowledge V. S. Sundaram and G. G. Kleiman, and Conselho Nacional de Pesquisa do Brasil, for the Pt-Cu(110) sample and for continuing collaboration. We appreciate the help of S. J. Oh in setting up an experiment on Pt-Cu(110), although that particular run turned out to be totally unproductive. This work was partially supported by National Science Foundation Grant No. INT-78-07268. The experiments were performed at the Stanford Synchrotron Radiation Laboratory, which is supported by the National Science Foundation through the Division of Materials Research (in cooperation with the U. S. Department of Energy).

*Present address: National Laboratory for High Energy Physics, Ohomachi, Tsukuba-gun, Ibaraki-ken 305, Japan.

[1]J. W. Cooper, Phys. Rev. 128, 681 (1962).

[2]I. Lindau, W. E. Spicer, J. N. Miller, D. T. Ling, P. Pianetta, P. W. Chye, and C. M. Garner, Phys. Scr. 16, 388 (1977).

[3]L. I. Johansson, I. Lindau, M. H. Hecht, S. M. Goldberg, and C. S. Fadley, Phys. Rev. B 20, 4126 (1979).

[4]L. I. Johansson, I. Lindau, M. H. Hecht, and E. Källne, Solid State Commun. 34, 83 (1980).

[5]The photoelectron energy distribution is taken to be representative of the electronic density of states.

[6]I. Lindau and W. E. Spicer, J. Electron Spectrosc. 3, 409 (1974).

[7]M. L. Shek, P. M. Stefan, D. L. Weissman-Wenocur, B. B. Pate, I. Lindau, and W. E. Spicer, J. Vac. Sci. Technol. 18, 533 (1981).

[8]M. L. Shek, P. M. Stefan, D. L. Weissman-Wenocur, B. B. Pate, I. Lindau, W. E. Spicer, and V. S. Sundaram, Surf. Sci. 115, L86 (1982).

[9]M. L. Shek, Ph.D. thesis, Stanford University, 1982 (unpublished).

[10]M. L. Shek, P. M. Stefan, I. Lindau, and W. E. Spicer, following paper, Phys. Rev. B 27, 7301 (1983).

[11]M. L. Shek, P. M. Stefan, I. Lindau, and W. E. Spicer, Surf. Sci. (in press).

[12]P. H. Citrin, G. K. Wertheim, and Y. Baer, Phys. Rev. Lett. 41, 1425 (1978).

[13]M. Mehta and C. S. Fadley, Phys. Rev. Lett. 39, 1569 (1977).

[14]P. Heimann and H. Neddermeyer, Phys. Rev. B 17, 427 (1978).

[15]P. Heimann, H. Neddermeyer, and H. F. Roloff, Phys. Rev. Lett. 37, 775 (1976).

[16]P. Heimann, H. Neddermeyer, and H. F. Roloff, J. Phys. C 10, L17 (1977).

[17]P. W. Chye, I. Lindau, P. Pianetta, C. M. Garner, and W. E. Spicer, Phys. Lett. 63A, 387 (1977).

[18]G. K. Wertheim, M. Campagna, and S. Hüfner, Phys. Condens. Matter 18, 133 (1974).

[19]D. H. Seib and W. E. Spicer, Phys. Rev. B 2, 1676 (1970).

[20]S. Hüfner, G. K. Wertheim, R. L. Cohen, and J. H. Wernick, Phys. Rev. Lett. 28, 488 (1972).

[21]M. L. Shek, P. M. Stefan, I. Lindau and W. E. Spicer, preceding paper, Phys. Rev. B 27, xxx (1983).

[22]F. C. Brown, R. Z. Bachrach, and N. Lien, Nucl. Instrum. Methods 152, 73 (1978).

[23]I. Lindau and W. E. Spicer, in *Stanford Synchrotron Radiation Research,* edited by S. Doniach and H. Winick (Plenum, New York, 1980), Chap. 6.

[24]Although the Cu 105-eV Auger transition has a surface sensitivity similar to that of the valence photoemission measurement, it is not used consistently because of its weak intensity for a small Cu concentration and also because of uncertainties due to electron backscattering from Pt.

[25]This is corrected by the electron collection angle by multiplying the electron escape depth by cos42°.

[26]M. L. Shek, P. M. Stefan, I. Lindau, and W. E. Spicer, Surf. Sci. (in press).

[27]W. Jost, *Diffusion in Solids, Liquids, Gases* (Academic, New York, 1952).

[28]These are only very approximate estimates of the mean penetration depths. The assumptions of a bulk diffusion coefficient (obtained for 13.9 at. % Cu in Pt) and a random diffusion process may be invalid for our diffusion conditions.

[29]In these difference spectra, the clean Pt(111) spectra are multiplied by the Pt concentration (estimated by AES) before they are subtracted from the PtCu(111) spectra.

[30]S. Hüfner, G. K. Wertheim, and D. N. E. Buchanan, Solid State Commun. 14, 1173 (1974).

[31]J. Stöhr, F. R. McFeely, G. Apai, P. S. Wehner, and D. A. Shirley, Phys. Rev. B 14, 4431 (1976).

[32]J. Stöhr, G. Apai, P. S. Wehner, F. R. McFeely, R. S. Williams, and D. A. Shirley, Phys. Rev. B 14, 5144 (1976).

[33]We have not investigated if any ordering occurs in these PtCu(111) samples. Even if there is, we expect only quantitative, and not qualitative, deviations from the analysis that follows.

[34]Since the bulklike layers below the topmost layer also contribute to the observed spectra, we should also consider the emission which is proportional to

$$x_{\mathrm{Cu}} \sum_{l=0}^{n} \frac{12!}{(12-l)!l!} x_{\mathrm{Cu}}^{l} (1-x_{\mathrm{Cu}})^{12-l} .$$

It turns out that the curves for $n=7$ and 8 follow very closely the curves for $m=5$ and 6, respectively, if they are also matched with experiment at 7.7 at. % Cu.

[35]G. G. Kleiman, V. S. Sundaram, C. L. Barreto, and J. D. Rogers, Solid State Commun. 32, 919 (1979).

[36]The evolution of the Pt 5*d* states as the Pt concentration changes has not been studied in this work. We have only noted the decrease of the Pt 5*d* states near E_F as Cu is incorporated into Pt(111). However, by analogy with other group-VIII–group-I*B* metals (Refs. 41, 42, and 45), it may be expected that, as the Pt concentration becomes small, most of the Pt 5d states would be pushed towards E_F and would also have a narrower width. For the case of 5 at. % Pt in Ag (Ref. 44), the Pt 5*d*–induced states lie between approximately −3.5 eV and E_F.

[37]S. Hüfner, G. K. Wertheim, and J. H. Wernick, Solid State Commun. 17, 1585 (1975).

[38]J. Hedman, M. Klasson, R. Nilsson, C. Nordling, M. F. Sorokina, O. I. Kljushnikov, S. A. Nemnonov, V. A. Trapeznikov, and V. G. Zyryanov, Phys. Scr. 4, 195 (1971).

[39]N. Mårtensson, R. Nyholm, H. Calén, J. Hedman, and B. Johansson, Phys. Rev. B 24, 1725 (1981).

[40]G. M. Stocks, R. W. Williams, and J. S. Faulkner, Phys. Rev. B 4, 4390 (1971).

[41]W. M. Temmerman, B. L. Gyorffy, and G. M. Stocks,

J. Phys. F 8, 2461 (1978).

[42]G. M. Stocks, R. W. Williams, and J. S. Faulkner, J. Phys. F 3, 1688 (1973).

[43]This is obscured by the low-energy cutoff in an early work [C. Norris and H. P. Myers, J. Phys. F 1, 62 (1971)] because the low photon energy used does not really permit a clear observation of the Ag subband.

[44]S. Hüfner, G. K. Wertheim, and J. H. Wernick, Phys. Rev. B 8, 4511 (1973).

[45]M. Pessa, H. Asonen, M. Lindroos, A. J. Pindor, B. L. Gyorffy, and W. Temmerman, J. Phys. F 11, L33 (1981).

[46]A. J. Pindor, W. M. Temmerman, B. L. Gyorffy, and G. M. Stocks, J. Phys. F 10, 2617 (1980).